S-band Radio Propagation Characteristics in Urban Environment for Unmanned Aircraft Systems

Fumie Ono, Kenichi Takizawa, Hiroyuki Tsuji, and Ryu Miura
Wireless Network Research Institute, National Institute of Information and Communication Technologies, NICT,
3-4, Hikarino-oka, Yokosuka, 239-0847 Japan
Email: fumie@nict.go.jp

***Abstract*—This paper describes the radio propagation characteristics in urban environment for a fixed-wing unmanned aircraft (UA) system. In the Great East-Japan Earthquake in 2011, the even the latest mobile phones became almost unavailable due to the breakdown of base stations, electricity outage, and traffic congestion. In addition, many areas in mountains or islands were isolated due to the damage of roads, harbors, and communication infrastructures. In such a situation, a UA system has a potential to provide temporal communication links to the isolated areas while monitoring the situation in the disaster area. Therefore, we have conducted a measurement campaign in order to characterize ground-to-air radio channels for small UA at several locations, including urban and non-urban environments. Some measurement results of ground-to-air link in urban environment are reported in this paper. It is demonstrated that there is a suitable flight altitude for long-range ground-to-air channel in terms of radio propagation.**

I. Introduction

In the past disasters such as Great Hanshin Earthquake, and more recently, Great East Japan Earthquake, some disaster areas in Japan were isolated. In such isolated areas, the transportation and communication systems have been interrupted. Even though many people left behind in the isolated areas have mobile phones and mobile terminals, they were disconnected as the backbone network as well as the base stations had broken down. As a consequence, there has been an increasing demand for robust wireless communication networks in Japan, and the usage of a small unmanned aircraft (UA) system is considered as a promising means. In the case of the large-scale disaster, UAs serve as bridges among the isolated ground stations (GS) or ground access points if UA has an on-board repeater in urban or non-urban areas. [1–4].

In an urban environment, the linkage between UAs and GS are subject to multi-path interference due to reflection, diffraction, and scattering between the transmitter and the receiver. Severe multi-path can result in a nearly complete crash of control and command signals, which may limit the UA operational area or even cause a loss of the UA. In [5], a Wi-Fi equipment is installed to measure radio channel characteristics in terms of both received signal strength and packet error rate in the ground-to-air links. In [6], a ray-tracing model is employed to analyze a power-delay profile for the ground-to-air channel in an urban environment. The paper [7] summarizes that the ground-to-air link is modeled as a two-ray model. Moreover, the paper [8] analyzes the air-to-ground channel under over-water and hilly terrain conditions. However, the measurement results in an urban environment has not been investigated well enough to design the radio propagation model and the flight plan of UA in Japan.

We have conducted a measurement campaign in order to characterize the ground-to-air radio channels in an urban environment. In this paper, we report the measurement results at Sendai city in Japan. Sendai city is the largest city in the Tohoku region in Japan, and the second largest city located in the north of Tokyo. In this measurement, the ground-to-air radio channels are characterized by a received signal strength in the center frequency of 2.3 GHz. From the measurement results, it will be shown that there is a suitable flight altitude in terms of radio propagation.

II. Measurement setup

Table I shows the specification of the small UA system employed in our measurement. Table II shows the specifications of the on-board transceivers and that of GS.

The urban area flights were conducted on July 29th, 2013 near Sendai-city. Figure 1 shows our measurement deployment. A snapshot of our experimental measurement setup is shown in Fig. 2. We use a UA and two GSs (denoted by GS1 and GS2). Sendai city is located between the two GSs. The GS2 was located at about 500 m from the flight area and the GS1 is separated by 11 km from GS2. For long-range line-of-sight (LOS) links, terrain clearance is the primary

TABLE I. Specification of unmannd-aircraft system

Wingspan, Weight	2.8 m, 5.9 kg
Payload	0.5 kg (Maximum)
Nominal endurance	about 2-3 hours
Control range	9 km
Wind speed limitation	25 kts (Maximum)
Flight altitude limitation	5 km (Maximum)
Flight speed	83 km/h
Driving power	Direct drive electric
Launch/Landing	Hand launch, Deep stall landing
Control	Manual/autonomous control

TABLE II. Specifications of on-board transceiver and ground station

Frequency	2 GHz (Experimental station)
Bandwidth	6 MHz
TX power	2 W
Moduation	MSK
Antenna of on-board transceiver	λ/4 whip antenna (gain:0 dBi)
Antenna of GS transceiver	Patch antenna (gain:9 dBi)
Weight of GS	about 6 kg (w/o power generator)
Weight of on-board transceiver	0.47 kg (w battery)
Battery life	about 2 hours
Range	20 km (Maximum)

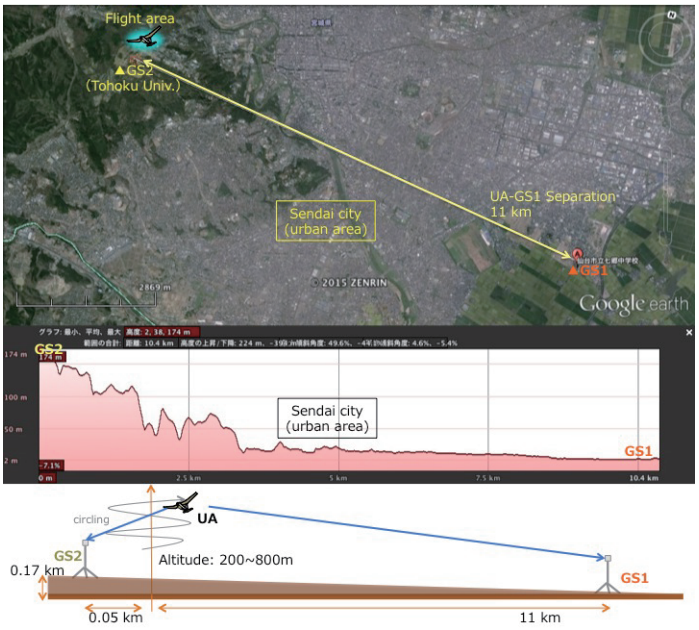

Fig. 1. Experimental deployment for ground-to-air radio propagation

Fig. 2. Snapshot of our measurement setup.

consideration in order to establish a reliable communication link. The clearance was secured between UA and GSs in this measurement deployment.

Each GS has a patch antenna with a gain $G_{\mathrm{g}} = 9$ dBi. The height of GS antennas is 0.15 m above the ground level. The GS2 antenna was set on 30 degree from geographic north in azimuth with 45 degree elevation angle. The GS1 antenna was set on 270 degree from geographic north in azimuth with 45 degree elevation angle. On the other hand, the UA is equipped with a $\lambda/4$ whip antenna with a gain $G_{\mathrm{a}} = 0$ dBi.

In this experiment, the center frequency of the transmitter was chosen as 2.3 GHz and the transmit power from GSs at antenna terminal was 33 dBm. The average power of thermal noise at the receiver is -105 dBm, which is equivalent to 2323 meters in the free space. The synchronization between the UA and GSs is accomplished by GPS signal. In the measurement, the received signal strength through the radio channels between GS and UA was recorded at the UA side.

III. Experimental Results

This section describes the flight trajectory and the flight attitude during the experimental measurement. Then, the measurement results are presented and discussed.

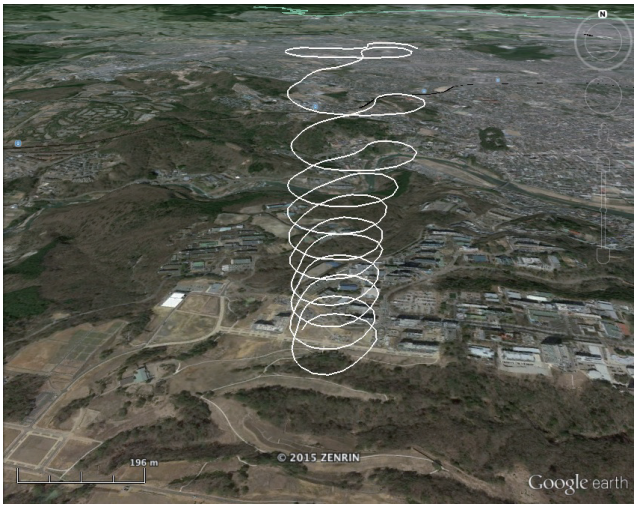

Fig. 3. Flight trajectory of small UA during the experimental measurement

A. Flight trajectory and flight attitude

Figure 3 shows a relative part of the flight trajectory of the UA for this experimental measurement. Moreover, the flight attitude of the UA during this measurement is shown in Fig.4.

In this experimental measurement, the UA circles around above the fixed area in order to keep the distance between GSs. The radius of circling of the UA is about 50 m. Since altitude against land (AGL) in typical operations of small UAs is expected in less than 1500 meters [9], the AGL throughout this measurements were set less than 1500 meters. In this experimental measurement, the UA was controlled to lower altitude while turning.

Figure 5 shows a part of the wind speed on the air and the wind direction relative to Fig.3. It was observed that the wind speed gradually increases as an increase of the flight altitude. As the wind speed increases, the flight of the UA becomes unstable. This results in the drastic change of the antenna pattern at the on-board transceiver change dramatically.

B. Radio propagation characteristics

Figures 6 and 7 show the received signal levels between GS2 and UA and between GS1 and UA. In these figures, the horizontal axis is the flight altitude and the vertical axis is the received signal level. The measured signal level is plotted with blue line, and the free-space path loss propagation model (denoted by model 1) and two-ray ground reflection model (denoted by model 2) are plotted with red lines.

For the free-space path loss propagation model, the received signal level of our experimental measurement is given by

$$\begin{aligned} P_{\mathrm{r}} =& P_{\mathrm{t}} + G_{\mathrm{a}}(p_{\mathrm{a}}, p_{\mathrm{g}}) + G_{\mathrm{g}}(p_{\mathrm{a}}, p_{\mathrm{g}}) \\ & - L_{\mathrm{a}} - L_{\mathrm{g}} - L_{\mathrm{path}}(d, h_{\mathrm{a}}, h_{\mathrm{g}}) \end{aligned} \tag{1}$$

where P_{t} is the transmission power, G_{a} is the antenna gain of UA that calculates by the radiation pattern considering the positions of UA and GS (p_{a} and p_{g}), G_{g} is the antenna gain of GS that calculates by the radiation pattern considering the positions of UA and GS (p_{a} and p_{g}), L_{a} and L_{g} are the loss

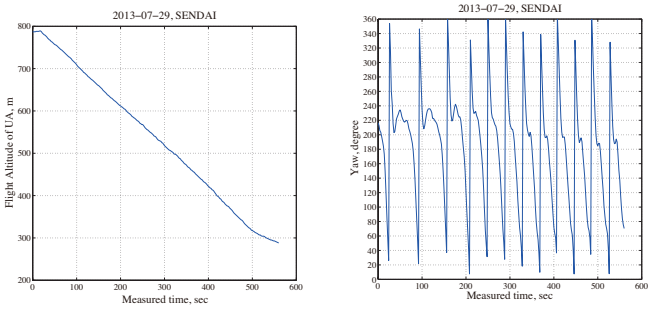

(a) Flight altitude of UA (b) Yaw of UA

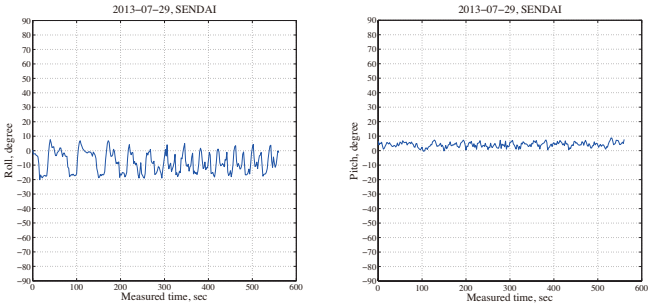

(c) Roll of UA (d) Pitch of UA

Fig. 4. Flight attitude during experimental measurement

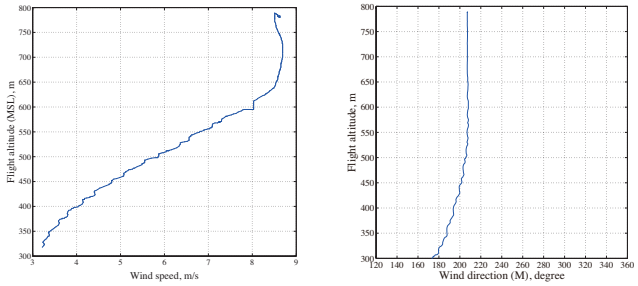

(a) Wind speed (b) Wind direction

Fig. 5. Wind direction and wind speed during the experimental measurement

at the UA and GS, and $L_{\mathrm{path}}(d, h_{\mathrm{a}}, h_{\mathrm{g}})$ is the path loss of the free space between UA and GS considering the height of antenna of UA and GS, h_{a} and h_{g}.

In the case of GS2 (for short-range measurement), the received signal level increases as the flight altitude of the UA decreases. Moreover, the received signal level changes within ± 1 dB since the UA is flying circularly.

On the other hand, in the case of GS1 (for long-range measurement), the received signal level is almost no changes even in the flight altitude increase since the distance between the UA and GS1 is long enough compared to the flight altitude. However, it is observed a height pattern regarding to the relationship between antenna height and electric field intensity occurs since the height of the GS antenna is fixed and that of the UA antenna is changed according to flight altitude. The

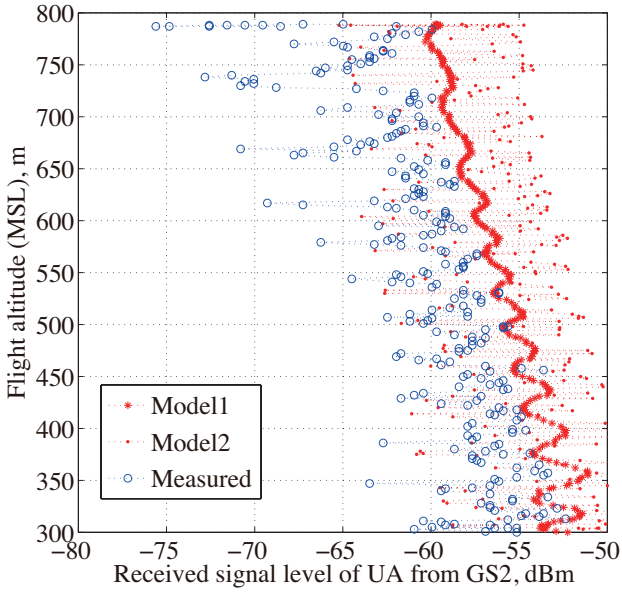

Fig. 6. The received signal level of GS2 (UA-GS2 separation is about 0.05 km)

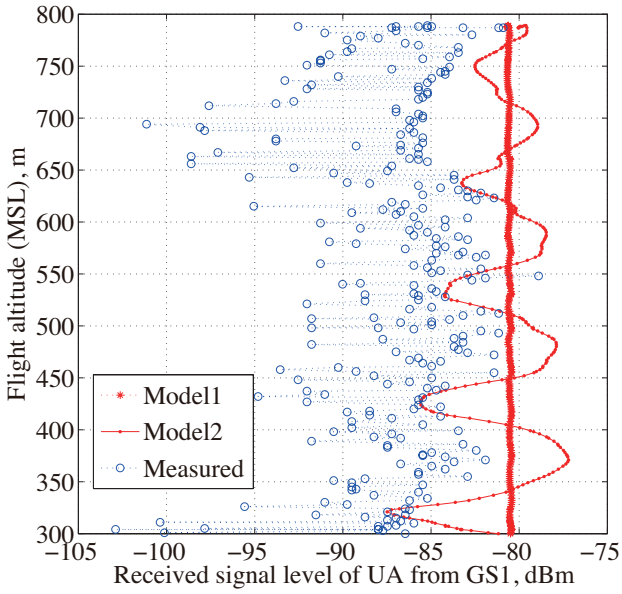

Fig. 7. The received signal level of GS1 (UA-GS1 separation is about 11 km)

theoretical pitch of the height pattern is given by

$$p_{\mathrm{H}} = \frac{\lambda d}{2h_{\mathrm{g}}} \tag{2}$$

where λ is the wave length. Here, if frequency is 2.3 GHz, the height of GS1 antenna, h_{g} is about 12 m and the distance between UA-GS1, d, is 11000 m, the height pattern pitch is about 60 m. The height pattern pitch of measured signal level is closer to about 60 m. From this figure, the desirable flight altitude for GS1 is expected to be from 450 m to 500 m in this measurement.

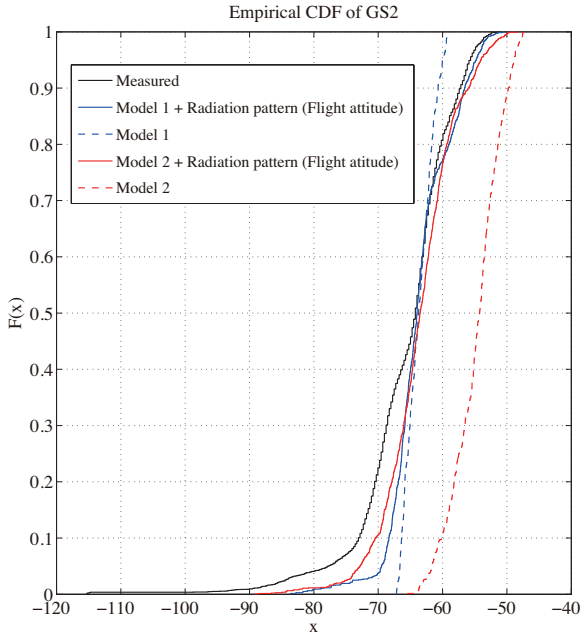

Fig. 8. The cumulative distribution function of the received signal from GS2

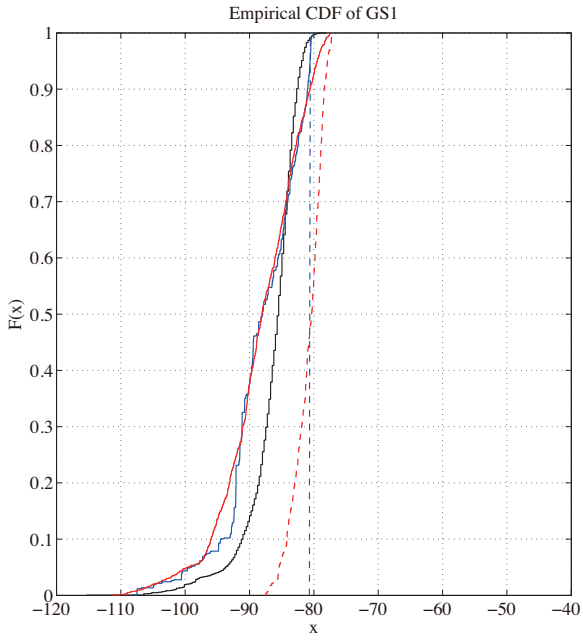

Fig. 9. The cumulative distribution function of the received signal from GS1

Figures 8 and 9 show the cumulative distribution functions of the received signal at GS2 and GS1. In these figures, the measured signal level is plotted with black line, model 1 are plotted with blue lines and model 2 are plotted with red lines. The blue and red solid lines are each model that calculates by the antenna gains, $G_{\mathrm{a}}(\theta_{\mathrm{roll}}, \theta_{\mathrm{pitch}}, \theta_{\mathrm{heding}}, p_{\mathrm{a}}, p_{\mathrm{g}})$ and $G_{\mathrm{g}}(p_{\mathrm{a}}, p_{\mathrm{g}})$, considering the flight attitude $(\theta_{\mathrm{roll}}, \theta_{\mathrm{pitch}}, \theta_{\mathrm{heding}})$ and positions of UA and GS (p_{a} and p_{g}). It is clear that the model 2 considering the flight attitude and the flight position is closer to the measured signal level.

IV. Conclusion

This paper described the overview of our experimental measurement for an unmanned aircraft system and reported some measurement results of the ground-to-air radio channel in an urban environment. The model of the measurement signal level approaches the two-ray model. In the case of a long-range LOS link, we observed that the height pattern regarding to the relationship between antenna height and electric field intensity. Throughout this experimental measurement, it was clarified that there is the suitable flight altitude in terms of radio propagation for long-range LOS link.

Acknowledgement

This research was conducted under a contract of R&D for radio resource enhancement, organized by the Ministry of Internal Affairs and Communications, Japan.

References

[1] D. Henkel and T. X. Brown, "On controlled node mobility in delay tolerant networks of unmanned aerial vehicles," in *International Symposium on Advance Radio Technolgoies (ISART)*, pp. 7–9, 2006.

[2] A. Jenkins, D. Henkel, and T. X. Brown, "Sensor data collection through gateways in a highly mobile mesh network," in *IEEE Wireless Communication Network Conference*, pp. 2786–2791, 2007.

[3] E. Yanmaz, "Connectivity versus area coverage in unmanned aerial vehicle networks," in *Communications (ICC), 2012 IEEE International Conference on*, pp. 719–723, 2012.

[4] F. Ono, H. Ochiai, K. Takizawa, M. Suzuki, and R. Miura, "Two-way relay networks using unmanned aircraft systems," in *Vehicular Technology Conference, 2013. VTC 2013-Spring. IEEE 77th*, 2013.

[5] E. Frew and T. Brown, "Airborne communication networks for small unmanned aircraft systems," *Proceedings of the IEEE*, vol. 96, no. 12, pp. 2008–2027, 2008.

[6] C. Cerasoli, "An analysis of unmanned airborne vehicle relay coverage in urban environments," in *Military Communications Conference, 2007. MILCOM 2007. IEEE*, pp. 1–7, Oct 2007.

[7] K. Takizawa, F. Ono, M. Suzuki, H. Tsuji, and R. Miura, "Measurement on s-band radio propagation characteristics for unmanned aircraft systems," in *Antennas and Propagation (EuCAP), 2014 8th European Conference on*, pp. 3068–3072, April 2014.

[8] D. W. Matolak and R. Sun, "Ag channel measurement and modeling results for over-water and hilly terrain conditions," *NASA/CR-2015-218486*, pp. 1–140, 4 2015.

[9] ITU-R, *Characteristics of unmanned aircraft systems and spectrum requirements to support their safe operation in non-segregated airspace*, Dec. 2009.